International Journal of Mathematics and Physical Sciences Research ISSN 2348-5736 (Online)
Vol. 2, Issue 2, pp: (95-105), Month: October 2014 – March 2015, Available at: www.researchpublish.com

Design and Simulation for Optimal Structure of Cross Type Capacitive Acceleration MEMS Sensor

Nguyen H. D. Khang[1], Duong T. Phuoc[2], Nguyen D. Giang[3], Truong H. Ly[4], Nguyen N. Viet[5]

[1]The University of Science, VNU-HCM
[2,5]R&D Center, Saigon High-Tech Park
[3,4]IC Design Research and Education Center, VNU-HCM
Ho Chi Minh City, Vietnam

Abstract: **This article focuses on the design and simulation for optimal structure of cross type capacitive acceleration MEMS sensor. The sensor structure is built by using analytic model combining with the emulation using Ansys Workbench. This structure must meet all production criteria: acceleration range is 0 – 10 g, the size is not over 12×12 mm^2, the resonant frequency is greater than 1 kHz, the damping coefficient range is [0.59 – 0.707], and the minimum sensitivity is 0.5 pF.**

Keywords: **MEMS, resonant frequency, damping coefficient, mass, ANSYS.**

I. INTRODUCTION

In MEMS technology, capacitive acceleration sensor has been widely used [1]. Compared with piezoelectric and piezoresistive types, capacitive acceleration sensor has higher sensitivity and stability [2-5]. The operation frequency range of this sensor depends on two parameters: its natural fluctuation frequency and damping coefficient. While increasing of the resonant frequency leads to decreasing of sensor sensitivity, the damping coefficient depends strongly on the characteristics of the sensor structure and the air layer surrounding the sensor [6]. Therefore, accurately assessing these criteria in order to determine the optimal structure for the sensor fabrication plays a decisive role.

Finding the optimal structure and simulating its working are important tasks for sensor designers. However, the simulation solely based on the finite element method through the random structures will take lots of time and is inefficient [7]. Analytic model allows to control more elements, but the result is less accurate with complex structures and variable conditions. Combining these two methods is preferred for the design of cross type capacitive acceleration sensor.

In this article, we propose four optimal models for cross type capacitive acceleration sensor. These models must meet the criteria of appropriate size, resonant frequency, sensitivity and damping coefficient. Finding the optimal structures are done by combining ANSYS software and analysis method. With the first three criteria, two analytic models have been proposed for the sensor structures. We then use ANSYS simulation to determine the suitable analytic model. This model is used to perform the loop calculations for finding the structures that meet these criteria. Finally, the satisfied structures are simulated by Ansys to figure out the suitable damping coefficient for the sensor.

II. IMPLEMENTATION METHODS

A. Analytic Models

The structure of capacitive acceleration sensor includes the mass block mounted to bracket by the hanging beams (Figure 1). The moving electrodes are formed on the surface of the vibrating block and separated from the fixed electrodes by a thin air layer. When there is external influence, the mass moves and causes changes of the distance between the capacitor plates and then changes of the capacitance. To increase the orientation, the capacitive acceleration sensor are structured in the multi – beam style. In order to increase the sensitivity and the capacitance value of the sensor, beside the single vibration block, there are compensation vibration block in mass corners.

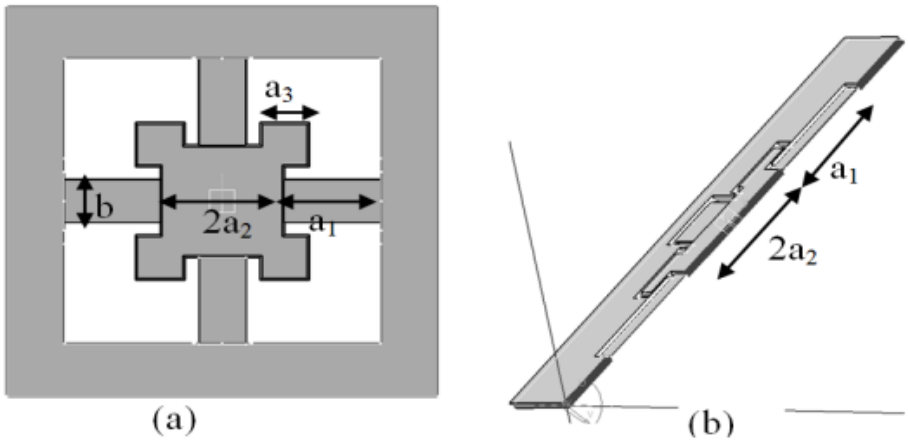

Fig. 1. The model of the acceleration sensor that is looked in a perpendicular direction to the sensor surface (a) and the sensor model is divided into 2 pieces in the cross section that is perpendicular to the sensor (b).

Based on the original structure, we propose two models for analyzing the elasticity for the capacity type acceleration sensor:

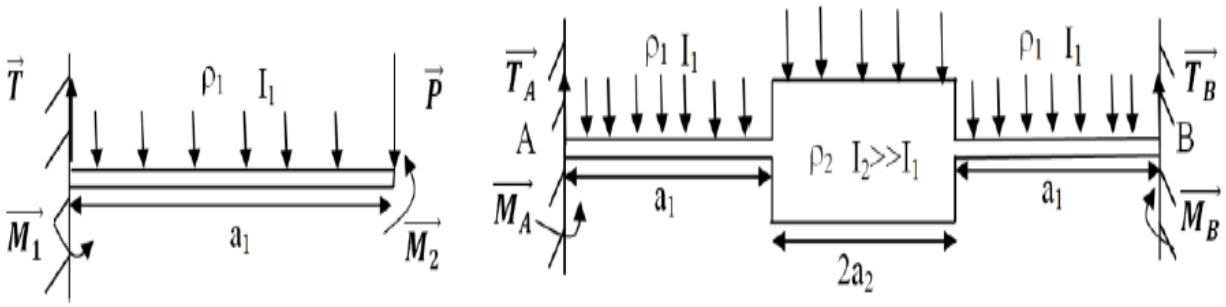

Fig. 2.Two models for analysing the elasticity for the capacity tye acceleration sensor: The capacitive acceleration sensor model with single beam and concentrating weight (a) and The capacitive acceleration sensor model with dual beam and contribution weight (b).

Model 1: The capacitive acceleration sensor model with single beam and concentrating weight (Figure 2a)

Conditions:

1. The beam is considered as the Bernoulli beam that one end is clamped at the bracket, and the other end is under concentrated force from the mass. At the head of beam, a bending momentum occurs against the deformation.
2. Ignoring the imperfection of wet etching, we consider mass as the rectangular block. The inertial momentum of the mass block is much larger than that of the beam. The displacement on the surface of mass block is constant.
3. Due to the symmetrical structure, we just consider ¼ the structure.

The performance equation:

The equilibrium equation for the power momentum for the section of the beam:

$$EI_1 w'' = -M \quad \textbf{(2.1)}$$

With:

$$M = M_1 + Tx - \int_0^x \rho_1 g(x-s)ds \quad \textbf{(2.2)}$$

The conditions for the force equilibrium:

$$T = \rho_1 a_1 g + P \quad \textbf{(2.3)}$$

The general solutions of the equation 2.4:

$$w = \frac{1}{EI_1}\left(-M\frac{x^2}{2} - T\frac{x^3}{6} + \frac{1}{24}\rho_1 x^4 + C_1 x + C_2\right) \quad \textbf{(2.4)}$$

The initial conditions:

$$\begin{cases} w'(x=0) = 0 \\ w'(x=a_1) = 0 \\ w(x=0) = 0 \end{cases} \Rightarrow \begin{cases} C_1 = 0 \\ C_2 = 0 \\ M = -T\frac{a_1}{2} + \frac{1}{6}\rho_1 g {a_1}^2 \end{cases} \quad \textbf{(2.5)}$$

in which:

E: Young Modulus.

I_1: inertial Moment.

w: deflect ion of beam.

M: reaction moment at cross section of beam.

ρ_1: density of beam distributed longitudinal direction.

T: reaction force at head of beam.

Model 2: Acceleration sensor of dual beam hanging the mass and contribution force (Figure 2b).

Conditions:

1. The mass includes the compentation weighting. The volume density in the length of the weighting 2a2 is a constant.
2. We consider mass as the rectangular block. The inertial momentum of the mass block is much larger than that of the beam. The displacement on the surface of the weighting is constant.
3. Only ½ structure is considered due to the symmerty.

The performance equation:

The equilibrium equation of the momentum for the cross section of the beam:

$$EI_1 w'' = -M \quad \textbf{(2.6)}$$

The components of the momentum due to the weight of the beam and the weighting:

$$\begin{cases} EI_1 {w''}_1 = -M_1 \\ M_1 = T_1 x - \int_0^x \rho_1 g(x-s)ds \end{cases} \quad \textbf{(2.7)}$$

The components of the momentum at the A end of the beam:

$$\begin{cases} EI_1 w"_2 = -M_2 \\ M_2 = M_A - T_2 x \end{cases} \quad \textbf{(2.8)}$$

The components of the momentum at the B end of the beam:

$$\begin{cases} EI_1 w"_3 = -M_3 \\ M_3 = -T_3 x \end{cases} \quad \textbf{(2.9)}$$

The conditions for the force equilibrium:

$$T_A = T_B = (\rho_1 a_1 + \rho_2 a_2) g \quad \textbf{(2.10)}$$

The solution of the equation 2.11:

$$w = w_1 + w_2 + w_3 \quad \textbf{(2.11)}$$

Boundary conditions:

$$\begin{cases} w'_1 + w'_2 + w'_3 \big|_{x=0} = 0 \\ w_1 + w_2 + w_3 \big|_{x=0} = 0 \\ w'_1 + w'_2 + w'_3 \big|_{x=2(a_1+a_2)} = 0 \\ w_1 + w_2 + w_3 \big|_{x=2(a_1+a_2)} = 0 \end{cases} \quad \textbf{(2.12)}$$

B. The model of couple field

The condition for the acceleration sensor to satify on a wide range of frequency (about more than 80% on its resonant frequency) while the error is assured to be within about 5% is that the damping ratio should be in the range of [0.59 – 0.707] (Figure 3). Therefore, the determination of the acceleration sensor structure with the appropriate damping ratio is very important.

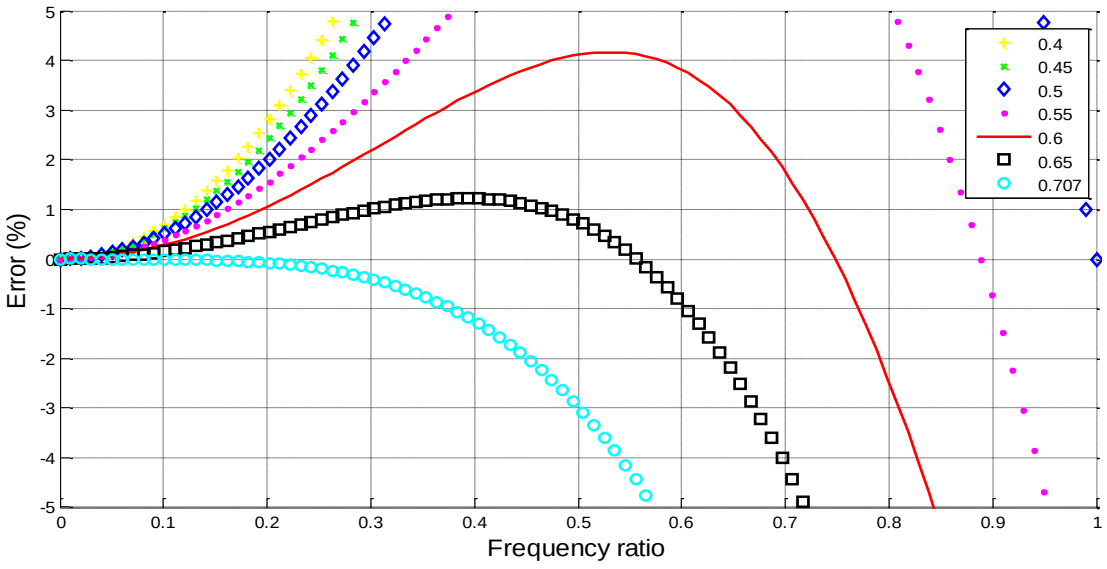

Fig. 3. The graph complies the error and the frequency ratio accordingly to the damping.

The energy during the fluctuation of the acceleration sensor is gradually dissipated due to the impact of surrounding air. Therefore, to determine the damping coefficient, we have to establish a model of interaction between the fluid (air) and the structure (the acceleration sensor) through FSI. The boundary conditions of the FSI simulation are described in Figure 4, the fluid boundary conditions consist of two wall boundaries replacing for the pyrex glass, the interface boundaries set at the contact surface of the sensor structure.

The conditions for the simulation:

1. The temperature is at 25°C.
2. Fluid is considered as laminar flow pattern.
3. The air is considered as the ideal gas.
4. The excess pressure is 0 atm.
5. The atmospheric pressure is 1 atm.
6. The speed of the initial air is 0 m/s.

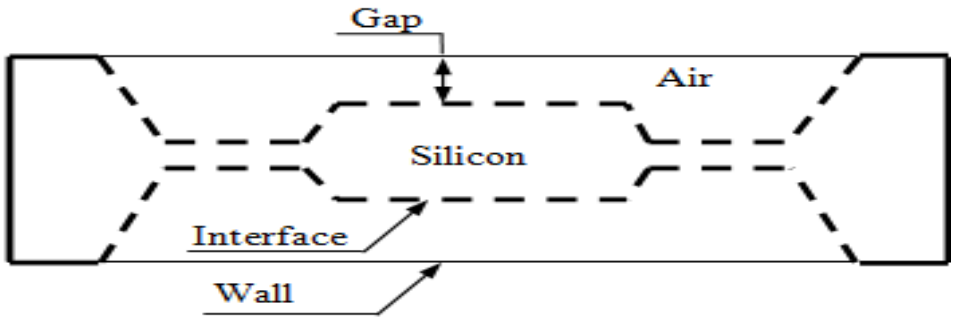

Fig. 4. The model of acceleration sensor interacts with the ambient air via the interfaces.

To investigate the influence of air on the operation of the acceleration sensor, we analyzed the energy dissipated through the damping factor of the signal obtained from the transition process of analysis (transients). The distance between the two surfaces of the electrode (gap) is changed in the process of analysis. The purpose of this work is to determine the appropriate gap that causes the criteria damping coefficient of 0.6 ~ 0.7.

Beside the damping coefficient, this process of analysis help us to identify the natural frequencies of the sensors in the ambient air as well as the squeeze factors that are specific for the obstruction of the air moving in a narrow space. The simulations uses the FSI solver in the environment of ANSYS Workbench through the Transient analysis module and the CFX fluid analysis module.

III. RESULTS

A. Optimizing structures with the criteria of natural frequencies, maximum stress and sensitivity

Assessing the accuracy of the proposed models, we built nine sample structures, the static and modal simulation based on finite element method was used to find the stress, the translocation and the resonant frequency of each sample (Table I).

TABLE I. ANALYSIS RESULTS OF THE STRESSES, THE TRANSLOCATIONS, THE NATURAL FREQUENCIES OF 9 MODELS OF ACCELERATION SENSOR

	BL[a] (μm)	BW[a] (μm)	BH[a] (μm)	MW[b] (μm)	MH[b] (μm)	MR[c] (μm)	Dis (μm)	Fre (Hz)
1	4000	1200	50	4800	265	0.2	0.087	1703
2	4000	1500	60	5000	270	0.3	0.087	1706
3	4000	2000	70	5200	275	0.4	0.055	2519
4	4500	1200	50	5000	270	0.4	0.298	920
5	4500	1500	60	5200	275	0.2	0.117	1445
6	4500	2000	70	4800	265	0.3	0.058	2120
7	5000	1200	60	4800	275	0.3	0.198	1132
8	5000	1500	70	5000	265	0.4	0.126	1424
9	5000	2000	50	5200	270	0.2	0.212	1099

[a]BL, BW, BL: length, width, height of the beam.

[b]MW, MH, MR: width, height of the weighting.

[c]The volume ratio for the compensation of the weighting.

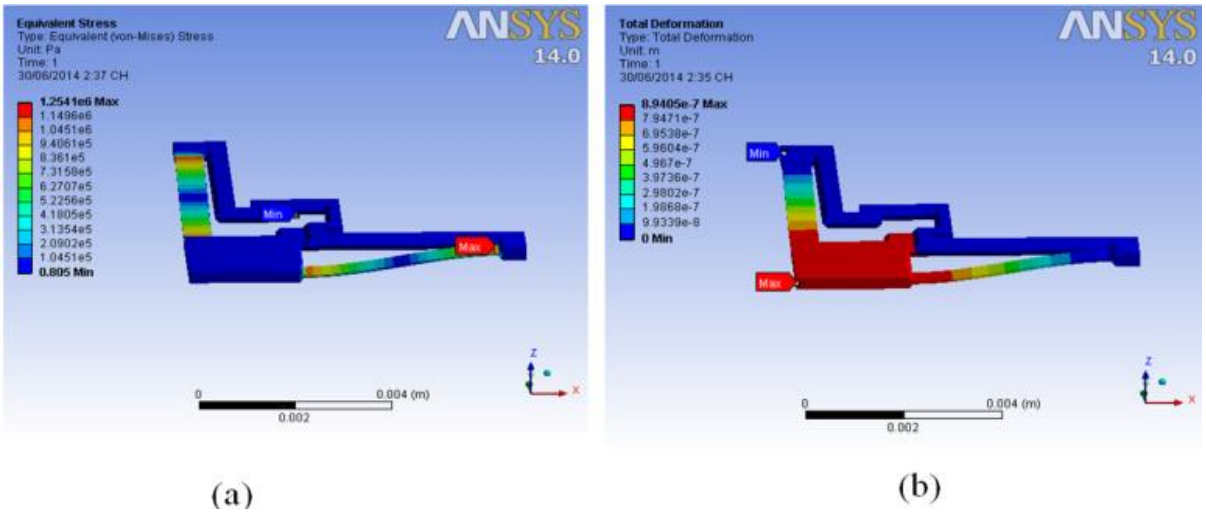

(a) (b)

Fig. 5. Graphic simulation results of the stress (a) and the translocation (b) when applying acceleration of 10g for sample structure 1.

The stress analyses through static simulation of sample structure 1 (Figure 5) has the highest value at the head of the beam and the lowest value at the middle of the beam. Under the external influence, the structure has different vibration modes corresponding with different frequencies. However, we only consider the first vibration mode containing the basic frequency for modal simulation, as other vibrations are harmonic frequencies and not essential values (Figure 6).

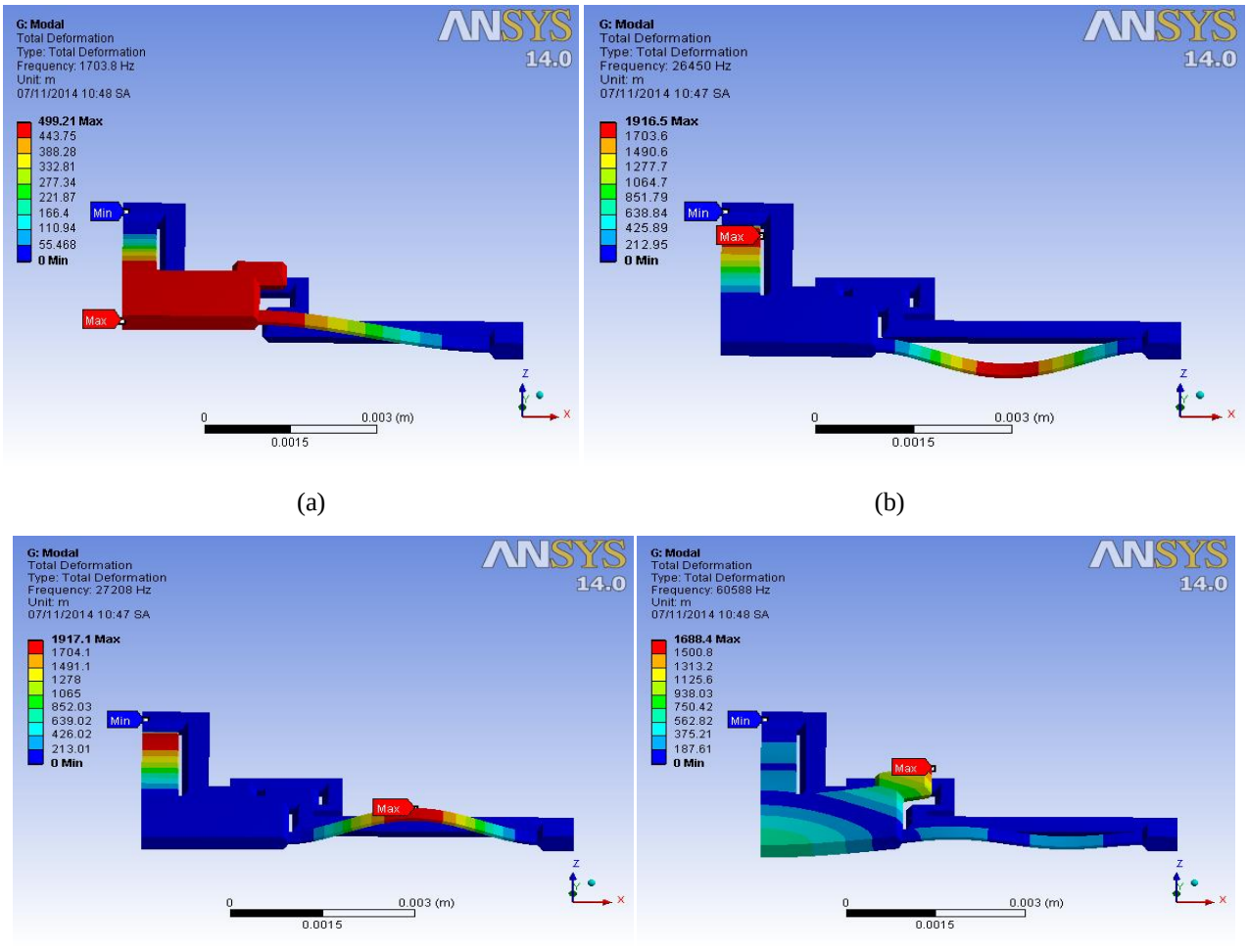

(a) (b)

(c) (d)

Fig. 6.Vibration mode shapes of sample structure 1.

With model 1, the displacement error is 14.4% and the resonant frequency error is about 5.9% (Table II). Comparing with model 2, the displacement error is 4.3%,and the resonant frequency error is 0.6% (Table III). Thus, in the two models, the model 2 has smaller error than that of model 1, and the errors do not exceed 5%. Considering the entire length of the beam, the translocation line of model 2 is closer the simulated values than that of model 1 (Figure 7). Therefore, model 2 is used more efficiently than model 1 when we determine the criteria of the size, the resonant frequency and the sensitivity of cross type capacitive acceleration sensor.

TABLE II. COMPARISON RESULTS OF MODEL 1 WITH ANALYSIS RESULTS BY ANSYS WORKBENCH

	Δ_1[d] (□m)	Δ_0[d] (□m)	ε_1 (%)	f_1[e] (Hz)	f_0[e] (Hz)	ε_2 (%)
1	0.077	0.087	13.5	1797	1703	5.5
2	0.077	0.087	13.8	1798	1706	5.4
3	0.047	0.055	18.0	2309	2519	8.3
4	0.275	0.298	8.4	951	920	3.4
5	0.106	0.117	10.4	1527	1445	5.7
6	0.047	0.058	23.0	2300	2120	8.5
7	0.177	0.198	11.9	1186	1132	4.7
8	0.109	0.126	15.6	1511	1424	6.1
9	0.185	0.212	14.6	1158	1099	5.4
Av.			**14.4**			**5.9**

[d]Δ_1, Δ_0: The displacement of the contact point of the beam and the mass block according to model 1 and the ansys simulation..

[e]f_1, f_0: The resonant frequency under analytic model 1 and the ansys simulation.

TABLE III. RESULTS COMPARISON OF MODEL 2 WITH ANALYSIS RESULTS BY ANSYS WORKBENCH

	Δ_2[f] (□m)	Δ_0[f] (□m)	ε_1 (%)	f_2[g] (Hz)	f_0[g] (Hz)	ε_2 (%)
1	0.083	0.087	5.2	1732	1703	1.7
2	0.083	0.087	5.4	1733	1706	1.6
3	0.051	0.055	7.5	2209	2519	12.3
4	0.288	0.298	3.3	928	920	0.9
5	0.120	0.117	2.1	1441	1445	0.3
6	0.054	0.058	6.7	2147	2120	1.3
7	0.191	0.198	3.7	1140	1132	0.7
8	0.119	0.126	5.5	1443	1424	1.3
9	0.206	0.212	3.1	1099	1099	0.0
Av.			**4.3**			**0.6**

[f]Δ_2, Δ_0: The displacement of the contact point of the beam and the mass block according to model 1 and the ansys simulation.

[g]f_2, f_0: The resonant frequency under analytic model 1 and the ansys simulation.

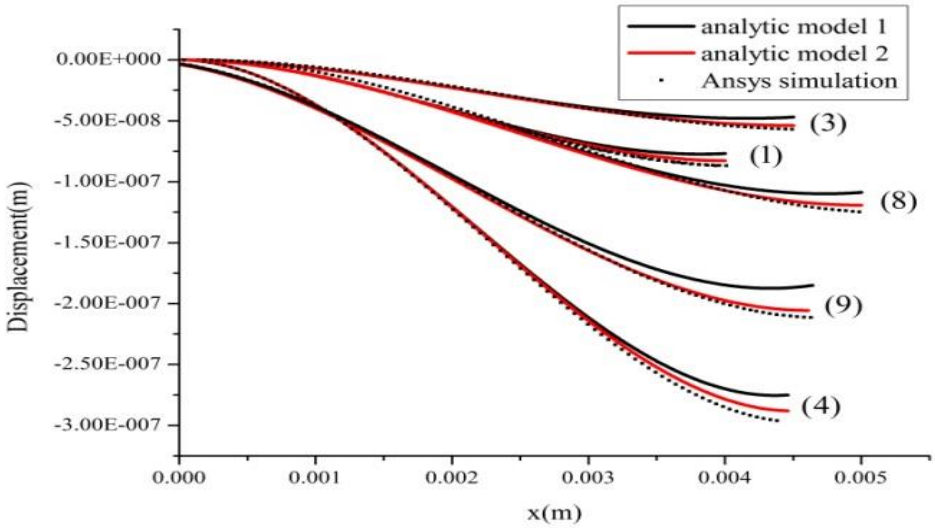

Fig. 7. The comparison of the performance line of the beam's translocation under Ansys simulation, analytic model 1, analytic model 2 of the structures 1, 3, 4 and 8 when applying 1g.

Based on the model 2, the structural parameters are determined based on the block diagram shown in Figure 8.

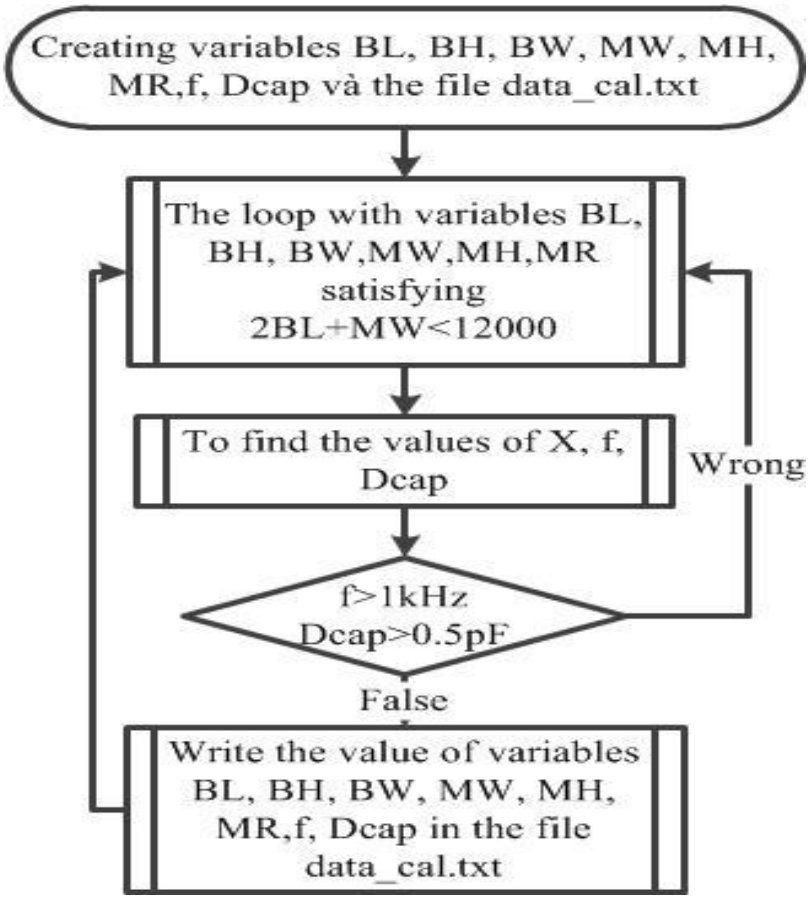

Fig. 8. The block diagram for finding the optimal structure for the three criteria of size, frequency and sensitivity.

The number of the structures that meets the three manufacturing criteria is about 31,000. In the manufacturing conditions, especially of wet etching, this leads to reduce the area of the electrode and increase the resonant frequency of the capacitive acceleration sensor. Therefore, we should give priority to selecting the structure with higher sensitivity. With the limit of this criterion, we selected four structures showed in Table IV.

TABLE IV. FOUR STRUCTURES FOR ACCELERATION SENSOR.

	Δ_2 (□m)	Δ_0 (□m)	ε_1 (%)	f_2 (Hz)	f_0 (Hz)	ε_2 (%)	ΔC_2 (pF)
1	0.193	0.201	4.0	1135	1118	1.5	5.99
2	0.122	0.129	5.4	1424	1404	1.4	4.16
3	0.073	0.077	5.1	1867	1820	2.6	2.21
4	0.191	0.186	2.7	1139	1158	1.6	2.23

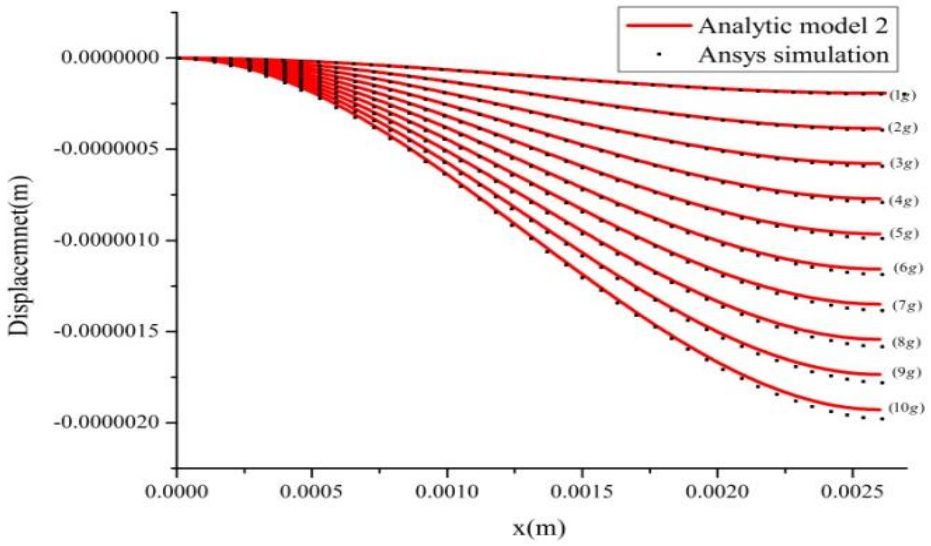

Fig. 9. The comparision graph of the translocations of the analytic models 1 and 2 and the simulation results of the optimal structure by Ansys Workbench 14.0 when the acceleration is [1g, 10g].

When simulating the results of the structures by Ansys Workbench, the result of the beam's displacement of the structure 1 is collected and shown in Figure 9. Compared with the analytic model 2, the displacement error is 4%, natural frequency error is 1.5%.

B. Optimizing the structures in the damping criterion –satisfying 5% error

The pressure distribution is consequence of interaction between structure and gas film. The different excess pressure in top and bottom surface is the main reason changing damping value.

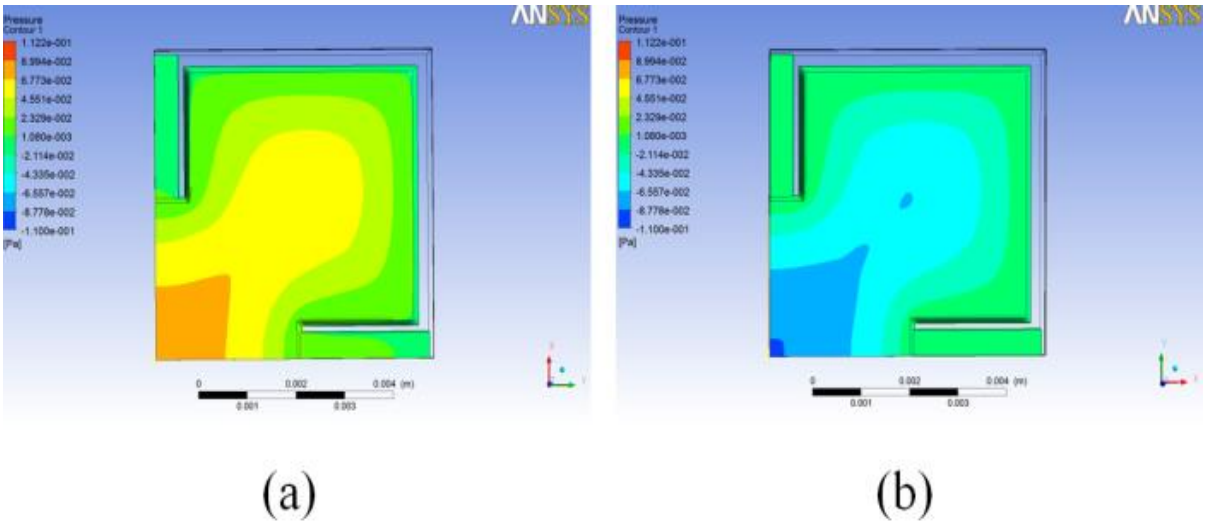

Fig. 10. The presure distribution in the top (a) and bottom (b) surface of optimal structure 3 under impact of squeeze film effect with gap 7.5 μm.

The chronologic translocation data since after the excitation of the fluctuation in the form of the harmonic with the fading amplitude is shown in Figure 11. When the initial value of gap thickness is smaller, the fluctuation amplitude of the mass block is reduced. By changing this parameter, the optimal structure for fabrication can be determined.

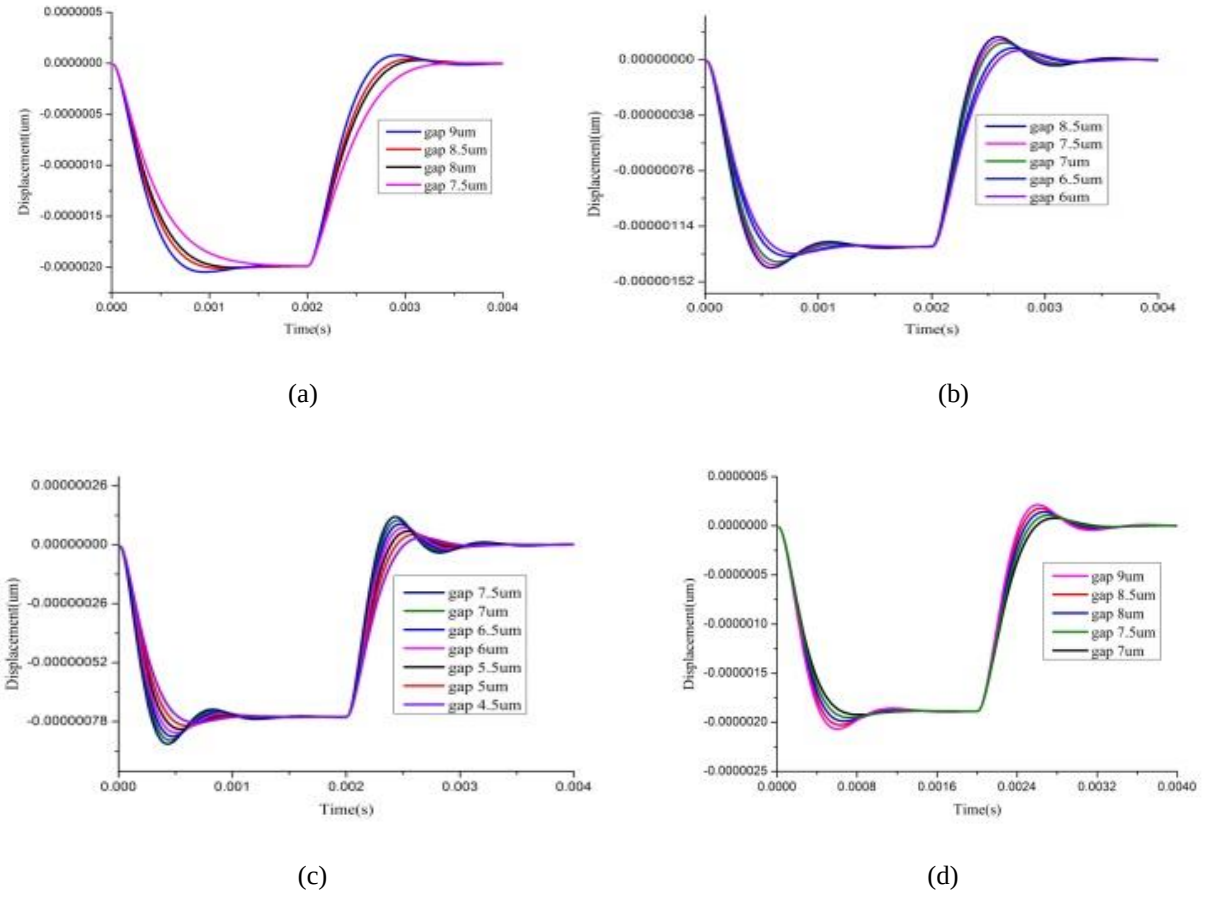

(a) (b)

(c) (d)

Fig. 11. The displacement graph of the acceleration sensor according to circumstances of changing the gap.

TABLE V. THE RESULTS OF THE FLUCTUATION THAT USE NONLINEAR REGRESSION FUCTION

Num.	h_0^h	$f_\zeta{}^i$	σ^j	ζ^k	**Num.**	h_0^h	$f_\zeta{}^i$	σ^j	ζ^k
Op1	7.5	417	2.6	0.866	**Op2**	6	552	6.4	0.703
	7.5	287	2.6	0.837		6.5	619	5.4	0.698
	8	612	2.2	0.684		7	680	4.7	0.668
	8	395	2.2	0.778		7.5	735	4.1	0.642
	8.5	645	2.0	0.652					
	9	707	1.8	0.570					
Op3	7.5	1193	4.2	0.494	**Op4**	7	632	1.6	0.714
	7	1139	4.8	0.525		7.5	694	1.4	0.677
	6.5	1077	5.5	0.559		8	750	1.2	0.639
	6	1005	6.5	0.596		8.5	798	1.1	0.603
	5.5	922	7.7	0.636		9	840	0.9	0.568
	5	825	9.4	0.678					
	4.5	721	11.6	0.722					

[h]Inital value of gap (gas film) thickness (μm).

[i]Damping frequency (Hz).

[j]Squeeze number.

[k]Damping coefficient.

To determine the specific damping coefficient values in corresponding to each gap distance, we use the regression function in the form of faded harmonic fluctuation. The results are presented in Table V.

Through the process of analyzing the displacement data, we can determine the appropriate damping coefficients by selecting the optimal gap distance for the fabrication of sensors. While the error criterion does not exceed 5%, the sensors operate on a wide range of frequencies, and the damping coefficient should lie in the range of [0.59 – 0.707].

IV. CONCLUSION

The results show that combines the capacitive acceleration sensor model of dual beam and contribution weight with the structural analysis in Ansys Workbench via the finite element method and the couple field FSI, the optimal structure for the acceleration sensor has been identified.

With these structures, the acceleration sensors have the size less than 11×11 mm^2, the resonant frequency is greater than 1.1 *kHz*, the damping coefficient is in the range of [0.59 – 0.707] and the smallest sensitivity is 2.21 *pF*. Identifying these structures brings the great meaning for the fabrication and application of acceleration sensors.

ACKNOWLEDGEMENT

We are grateful to the support of the fund of HCMC Department of Science and Technology that have created all conditions for us to complete this article.

REFERENCES

[1] S. Middelhoek, "Handbook of sensors and actuators", Elsevier, Vol. 8, 2000, pp. 87-137.

[2] S.J. Sherman, W.K. Tsang, T.A. Core and D.E. Quinn, "A low cost monolithic accelerometers", VLSI Symp, 1992, pp. 34-35.

[3] N. Yazdi and K. Najafi, "A high sensitivity silicon accelerometer with a folded electrode structure", Journal of microelectromechanical systems, Vol. 12, 2003, pp. 479-486.

[4] W. Kuehnel and S.J. Sherman, "A surface micromachined silicon accelerometer with "on chip" detection circuitry", Vol. 45, Sensors and Actuators A: Physical, 1994, pp. 7-16.

[5] Y. Matsumoto, M. Iwakiri and H. Tanaka, "A capacitive accelerometer using SDB-SOI Structure", Sensors and Actuators A: Physical, 1996, pp. 267-272.

[6] S.J. Sherman and W.K. Tsang et al, "A low cost monolithic accelerometer: product/ technology update", IEEE Proceedings of the IEDM , 1992, pp. 501-504.

[7] C.T. Leondes, "MEMS/NEMS: Handbook techniques and applications", Springter science & business media, August 2008, pp. 325-335.